Influence of Al_2O_3 Level in CaO-SiO_2-MgO-Al_2O_3 Refining Slags on Slag/Magnesia-Doloma Refractory Interactions

LIUGANG CHEN, ANNELIES MALFLIET, PETER TOM JONES, BART BLANPAIN, and MUXING GUO

The influence of the Al_2O_3 level in CaO-SiO_2-MgO-Al_2O_3 (CSMA) stainless steel refining slags on the degradation of magnesia-doloma refractories was investigated through static refractory finger corrosion tests. The tests were performed at 1620 °C under Ar atmosphere, using slags with Al_2O_3 contents of 5, 10, and 20 wt pct, respectively. The results indicate that the formation of $2CaO{\cdot}SiO_2$ at the slag/refractory interface was suppressed by increasing the Al_2O_3 content to 20 wt pct, thereby changing the corrosion mechanism from an indirect dissolution to a direct dissolution of CaO and MgO from the refractories. The increased solubility limit of MgO by the Al_2O_3-rich CSMA slags results in an overall higher corrosion rate of the MgO-doloma refractory.

https://doi.org/10.1007/s11663-019-01596-y

I. INTRODUCTION

MAGNESIA-DOLOMA (or magnesia-dolomite) refractories are commonly applied in linings of stainless steelmaking units,[1–3] *e.g.*, argon oxygen decarburization (AOD) and vacuum oxygen decarburization (VOD) ladles. This is because of the advantages of magnesia-doloma refractories, such as the low cost and their inherent stability in contact with very basic slags that are used to remove impurities such as S and P.[1,4] As a result of the worldwide adoption of magnesia-doloma refractories, a multitude of studies on the wear mechanisms of this refractory type have been reported.[5–10] Le Coq *et al.*[5] investigated the corrosion behavior of doloma-carbon refractories by CaO-SiO_2-Al_2O_3-MgO-MnO-FeO-CaF_2 slags (CaO/SiO_2 ratio: 3.5 to 4.0, Al_2O_3: 28.2 to 32.0 wt pct) at 1600 °C. It was concluded from their results that the main corrosion mechanisms of the refractories are the interaction between lime and slags producing calcium aluminates and calcium silicates, followed by the slag infiltration into the refractories and the dissolution of periclase grains into the slag. Similar conclusions were drawn by Jasson *et al.*,[7] who investigated the dissolution of doloma-based refractories in liquid CaO-Al_2O_3-SiO_2-MgO slags with CaO/SiO_2 ratios of 4.8 to 5.2 and Al_2O_3 contents of 30 to 33 wt pct, at temperatures ranging from 1773 K to 1923 K. When the magnesia-doloma refractories are contacted by these CaO-SiO_2–containing slags, the formation of a $2CaO{\cdot}SiO_2$ (C_2S) layer at the slag/refractory interface is expected.[1,6,10] The formation of such a C_2S layer can retard the dissolution of refractory components into the slag and the infiltration of slag into the bulk refractory, thus mitigating the magnesia-doloma refractory corrosion. However, the formation of this protective C_2S layer can be strongly influenced by the chemical composition and physical properties of the slag. It is reported by Satyoko and Lee[11] that C_2S can form a discontinuous layer due to the simultaneous formation of low melting phases of magnesiowüstite (Fe,Mg)O and dicalcium ferrite ($2CaO{\cdot}Fe_2O_3$) from the interaction between dolomite and the stagnant molten CaO-SiO_2-FeO-MnO-MgO slags at 1350 °C. Park *et al.*[6] reported that for static conditions, the thickness of the C_2S layer is reduced by increasing the CaF_2 content in CaO-SiO_2-MgO-CaF_2 slags at 1893 K, because the slag viscosity is lowered with the increase of the CaF_2 level in the liquid slag. Besides the decreased slag viscosity, a high CaO solubility caused by the increased CaF_2 content in the slag could also be a reason for destabilization of the formed C_2S layer.[6]

In stainless steel refining (*e.g.*, AOD or VOD), CaF_2 is traditionally used to increase the solubility of lime into the molten slag and the slag fluidity, thereby not only improving steel refining kinetics but also the desulfurization thermodynamics through the higher sulfur

LIUGANG CHEN, ANNELIES MALFLIET, PETER TOM JONES, BART BLANPAIN, and MUXING GUO are with the Department of Materials Engineering, KU Leuven, BE-3001 Leuven, Belgium. Contact email: liugang.chen@kuleuven.be
Manuscript submitted November 15, 2018.
Article published online May 13, 2019.

capacity of the slags. However, the use of CaF_2 in stainless steel plants is being evaluated, as environmental concerns are growing.[12] This situation encourages the stainless steel industry to find substitutes for CaF_2 and to develop a fluoride-free slag. Al_2O_3 is particularly interesting to meet this metallurgical requirement, as elevated Al_2O_3 levels can increase the lime solubility and, hence, the sulfide capacity of the slag.[13,14] The addition of Al_2O_3 in the stainless steel refining slags, on the other hand, can influence the corrosion mechanisms of the magnesia-doloma refractory linings. It is reported that higher Al_2O_3 levels may favor the formation of $MgAl_2O_4$-based spinel solid solution ((Mg,Fe)(Al,Cr,-Fe)$_2O_4$) at high temperatures, changing the corrosion mechanism from direct dissolution to a slower indirect dissolution of periclase into the slag.[13,14] The effect of Al_2O_3 on the formation of the protective C_2S layer, however, has not yet been studied. Therefore, it is important to quantify the effect of the Al_2O_3 content in stainless steel refining slags on the degradation of magnesia-doloma refractories.

The influence of the Al_2O_3 content in CaF_2-free $CaO-SiO_2-MgO-Al_2O_3$ (CSMA) slags on the magnesia-doloma refractories corrosion is investigated in the present article. This is performed through static refractory finger corrosion tests at 1620 °C with Al_2O_3 content in the slag varying from 5 to 20 wt pct. The impact of the Al_2O_3 level in CSMA slags on the degradation of magnesia-doloma refractories was studied by characterization of corroded microstructures using a scanning electron microscope (SEM) and electron probe microanalysis (EPMA).

II. EXPERIMENTAL METHOD

A. *Materials Preparation*

The slags used in this work were synthesized from reagent grade SiO_2 (> 98.0 wt pct, supplied by Sibelco Benelux), MgO (99.9 wt pct, supplied by Alfa Aesar), Al_2O_3 (> 99 wt pct, supplied by Sasol North America, Inc.), and CaO calcined from $CaCO_3$ (99.8 wt pct, supplied by Sigma Aldrich) at 1000 °C for 24 hours. They were prepared by mixing dried oxide powders for 24 hours with alumina milling balls in a shake milling device. After homogeneously mixing, the obtained mixtures were filled in a Pt crucible and heated in an electrical resistance furnace (with bottom loading device) under Ar atmosphere at 1600 °C for 1 hour. The slags were subsequently quenched on a steel plate and crushed to powder. The composition of the synthetic slags is presented in Table I.

Table I. Compositions of the Synthetic Slags before the Refractory Finger Corrosion Tests (Weight Percent)

Test Number	CaO	SiO_2	MgO	Al_2O_3	C/S
A05	52.5	37.5	5.0	5.0	1.4
A10	49.6	35.4	5.0	10.0	1.4
A20	43.8	31.3	5.0	20.0	1.4

Cylindrical magnesia-doloma (MgO-doloma) refractory finger samples were provided by a steelmaking company (diameter = 15 mm, length = ~ 50 mm). Table II shows the chemical composition and cold crushing strength of the as-delivered MgO-doloma refractory specimens.

B. *Experimental Setup and Procedure*

Figure 1 shows the experimental apparatus for the static refractory finger corrosion tests. The details for the experimental setup were previously reported.[15] Molybdenum wires were used due to the high testing temperature. Around 150 grams of the synthetic slag were filled in a Mo crucible (with an inside diameter of 40 mm and height of 80 mm) and melted at 1620 °C in a high-temperature vertical tube furnace (GERO HTRV 100-250/18, with $MoSi_2$ heating elements). Purified argon gas (passing the gas through silica gel and a Mg turnings furnace operating at 500 °C to remove traces of moisture and oxygen) was blown into the furnace tube with a flow rate of 0.25 L/min to simulate the protective atmosphere in the industrial AOD operation process. The oxygen partial pressure was measured in the outlet of the Ar gas with a value of lower than 10^{-16} atm (Rapidox 2100, Cambridge Sensotec Ltd.). A cylindrical magnesia-doloma finger was fixed on a molybdenum wire with a diameter of 3 mm (Figure 1(b)) and held near the top of the furnace tube. After the slag was heated to 1620 °C and held for 60 minutes, a slag sample was taken by dipping an alumina rod into the molten slag, withdrawing the rod from the furnace (Figure 1(a)), and quenching it in air. Subsequently, the refractory finger was lowered and maintained at a position of 50 mm from the top of the Mo crucible for 10 minutes to preheat the finger. Afterward, the refractory finger was immersed into the molten slag for 120 minutes. After immersion, the refractory finger was immediately taken out of the furnace and cooled under an Ar stream, followed by a second slag sampling.

C. *Sample Analysis Techniques*

The tested refractory fingers were subjected to both macroanalysis of the refractory wear and microstructural analysis. For each refractory finger, the central area of the submerged part of the samples was extracted for microstructural assessment (Figure 1(c)). In order to avoid disintegration of the MgO-doloma sample, the refractory and slag samples recovered from the corrosion tests were immediately embedded in low viscosity resin (Epofix) by vacuum impregnation, ground with diamond plates, and polished with diamond paste using acetone, in order to avoid the hydration of magnesia and doloma. The polished samples were coated with a carbon layer for microstructural and compositional analyses. The microstructures of the corroded refractory samples were characterized using a high-resolution SEM (Philips XL-40 LaB_6) equipped with an energy-dispersive spectroscope (EDS, energy-dispersive X-ray analysis) with an ultrathin window. Compositional analyses of slag samples before and after corrosion tests were

Table II. Composition and Properties of the Investigated Direct-Bonded Magnesia-Doloma Refractory

Overall Composition (Weight Percent)				
MgO	CaO	SiO_2	Al_2O_3	Cold Crushing Strength (MPa)
55.0	33.2	1.2	0.5	60.0 to 65.0

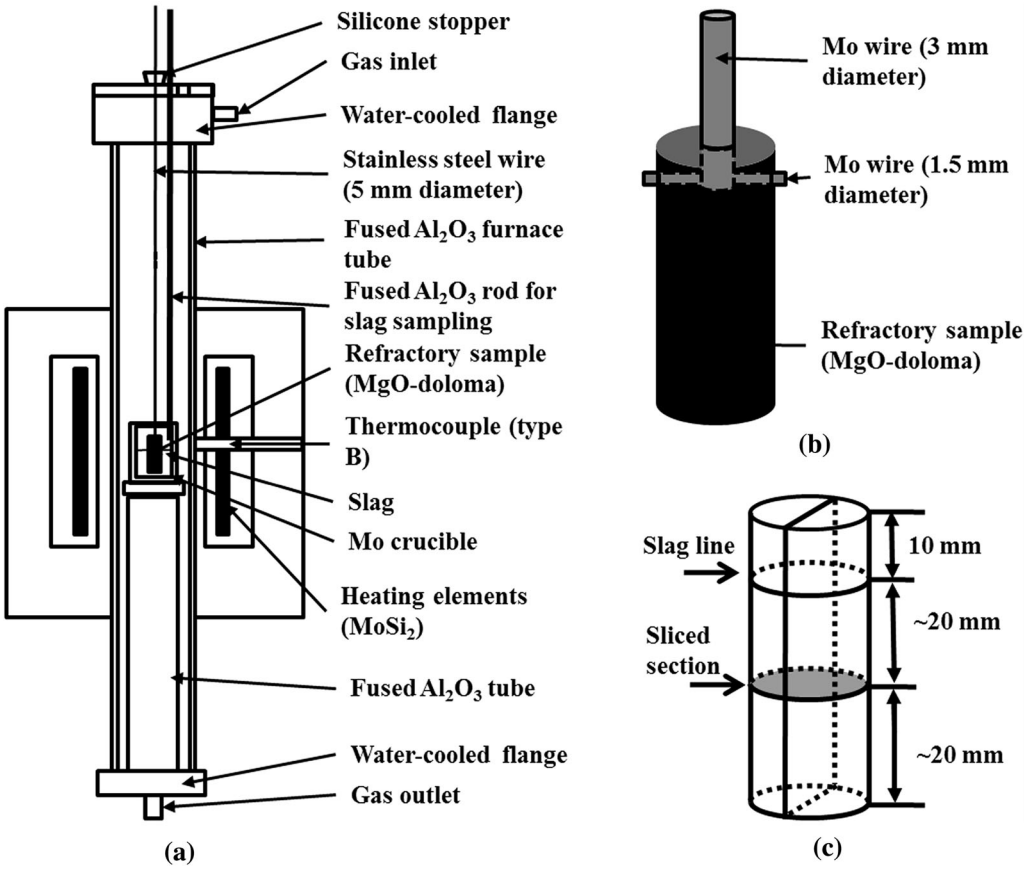

Fig. 1—Schematic drawings of (*a*) the vertical tube furnace for the static refractory finger corrosion tests, (*b*) the connection between the Mo wire and the refractory sample, and (*c*) the sample extraction scheme for microstructural assessment.

measured using EPMA with standardized wavelength dispersive spectroscopy (EPMA-WDS, ARL SEMQ 34). The results were obtained from at least four global analyses of the bulk slag areas (selected scans covering ~ 2500 μm^2 per analysis).

D. *Methodology of Thermodynamic Calculation*

Thermodynamic calculations were performed with FactSage software (version 7.0).[16] Phase diagram and equilibrium calculations were chosen to predict the dissolution of CaO and MgO and the reaction path between CaO or MgO particles and CSMA slags as a function of Al_2O_3 content in the slag at 1620 °C. The equilibrium calculations were performed with the equilibrium module EQUILIB, which is based on the minimization of the Gibbs free energy, and the Fact PS and FT oxide databases. Pure solids and the following possible solution phases were chosen in the calculations: (1) FT oxide-slag (molten oxide phase), (2) FT oxide-monoxide (oxide solid solution), (3) FT oxide-spinel (spinel solid solution), (4) FT oxide-α-Ca_2SiO_4 (α-Ca_2SiO_4 solid solution), (5) FT oxide-melilite (melilite solid solution), and (6) FT oxide-mullite (mullite solid solution), based on the phase analyses of CSMA systems at 1620 °C.[17] The dissolution of CaO and MgO and the interaction between the CaO or MgO particle and CSMA slags were modeled by the relative addition of pure CaO or MgO (x, in grams) into the slags ($(100 - x)$, in grams). The solubility limit of CaO or MgO in the CSMA slag was calculated according to the same approach reported for MgO or Al_2O_3 in previous work.[18,19] The maximum dissolution amount of CaO or MgO into the CSMA slag, which is defined as

the solubility limit of CaO or MgO, is determined with corresponding CaO- or MgO-bearing solid phase precipitates from the liquid slag. The slag compositions for the calculations were taken from Table I.

III. RESULTS

A. *Microstructure of the As-Delivered MgO-Doloma Refractory*

Figure 2 shows backscattered electron (BSE) images of the as-delivered magnesia-doloma (MgO-doloma) refractory sample. The investigated MgO-doloma brick is a direct-bonded mixture of the sintered periclase grains and sintered doloma grains. The chemical compositions of the related phases are listed in Table III. Periclase grains appear dark gray in the BSE mode, with a maximum grain size of around 700 μm (Figure 2(a)). A network formed by the high melting point $3CaO{\cdot}SiO_2$ (C3S) phase containing 68.8 ± 0.6 wt pct CaO, 4.2 ± 0.6 wt pct MgO, and 26.8 ± 0.6 wt pct SiO_2, as determined by SEM-EDS, can be observed in these periclase grains (Figure 2(b)). Doloma grains exhibit a larger grain size and are composed of a CaO matrix with dispersed MgO particles due to the limited mutual solubility between MgO and CaO in the solid state[20] (Figure 2(c)). The cracks and pores form a network in the MgO-doloma refractory.

B. *General Overview*

1. *Macroscopic observation*

The wear depth (Δd) of the refractory samples is determined by subtracting the final finger diameter (d_t) and twice the average adhered slag layer thickness (δ_{SL}) from the initial diameter (d_0) at the middle position of the submerged part of the specimens (Eq. [1]). The refractory finger diameter and slag layer thickness were measured using the Vernier scale and SEM, respectively:

$$\text{Wear depth} = \frac{1}{2}(d_0 - d_t - 2\delta_{SL}) \qquad [1]$$

Figure 3 shows the wear depths (millimeters) of the MgO-doloma refractory fingers in the CSMA slags. The wear depth gradually increases from 0.05 mm from test A05 (5 wt pct Al_2O_3) to 1.38 mm from A10 and 1.78 mm from A20. The results clearly indicate that the refractory wear is accelerated with increasing Al_2O_3 levels in CSMA slags.

Table IV shows the chemical composition of the CSMA slag before and after the finger tests. As shown in Table IV, the influence of the Al_2O_3 level in CSMA slags on the corrosion of MgO-doloma refractories can be evaluated by comparing the increase of the CaO and MgO content in the slags after testing. The increase of the CaO content is 1.0, 1.1, and 1.2 wt pct from tests A05, A10, and A20, respectively. In comparison, the

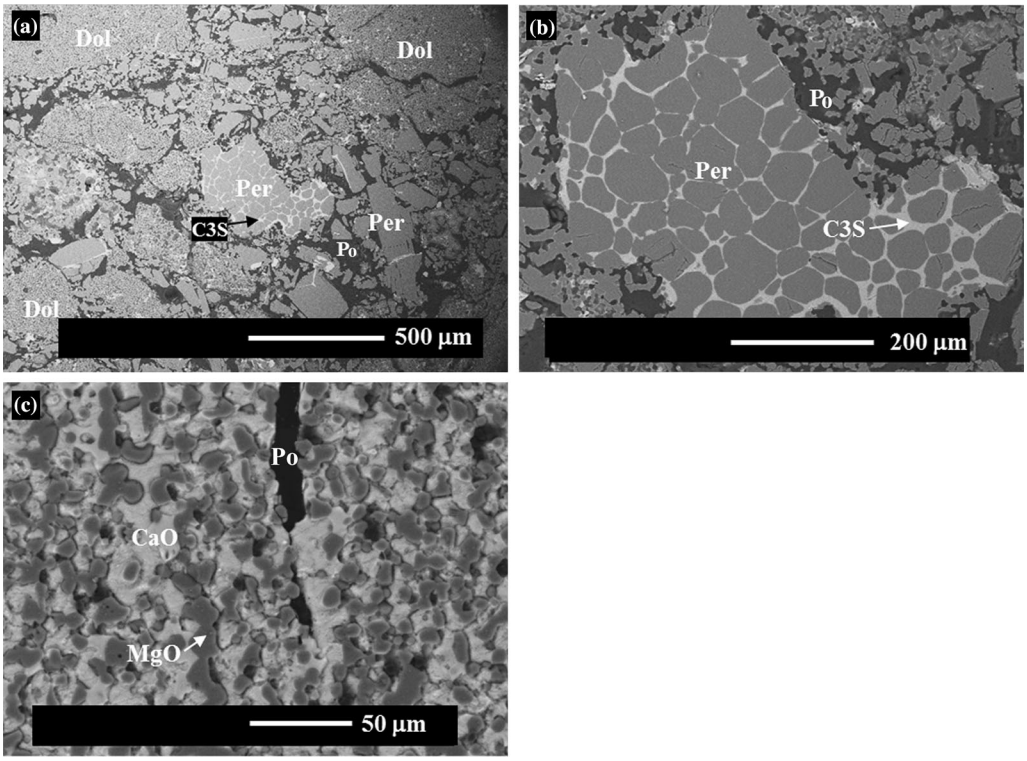

Fig. 2—Microstructure of the as-delivered magnesia-doloma brick: (*a*) microstructural overview; (*b*) sintered periclase grains; and (*c*) distribution of CaO and MgO in doloma grains: Dol = doloma grain, Per = magnesia (periclase), C3S = $3CaO{\cdot}SiO_2$, and Po = pore.

increase of the MgO concentration is 0.0, 1.4, and 3.4 wt pct in the tested CSMA slags with 5, 10, and 20 wt pct of Al_2O_3, respectively. The results indicate that the dissolution of CaO does not differ much, whereas the MgO dissolution was favored by increasing the Al_2O_3 level in CSMA slags. This result is in line with the wear rate of MgO-doloma refractories, illustrating the increased corrosion rate of MgO-doloma refractories by increasing Al_2O_3 concentration in CSMA slags (Figure 3).

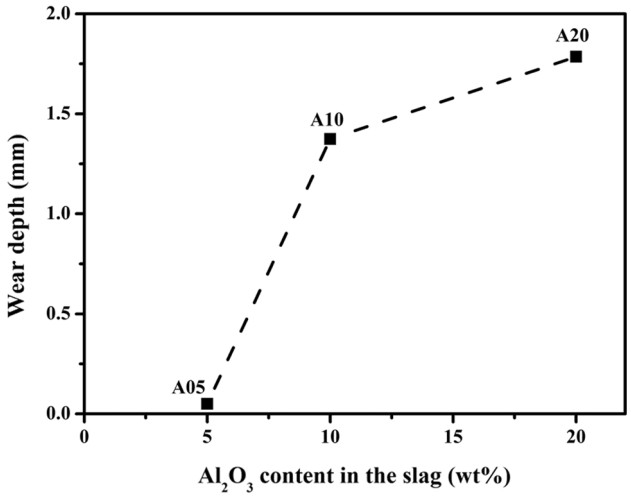

Fig. 3—Wear rates of the refractory fingers as a function of Al_2O_3 levels in the CSMA slag.

C. *Microstructural Observation*

Microstructures of the worn refractory samples are shown in Figure 4. A layer of frozen slag ("SL" in Figure 4(a)) with $2CaO{\cdot}SiO_2$ ("C2S" in Figure 4(a)) was observed on the surfaces of the samples from tests A05 and A10. Energy-dispersive spectroscopy area analyses of the attached slag layer are given in Table V. The thickness of this adhered "slag + C2S" layer gradually decreases from ~ 550 μm in test A05 to ~ 400 μm in test A10 and is absent in the sample of test A20, attributable to the fact that increasing the Al_2O_3 concentration in the CSMA slag lowers the slag viscosity. The MgO content in the frozen slag layer augments from 6.2 to 12.5 wt pct with increasing the Al_2O_3 level from 5 to 10 wt pct. As shown in Figure 4(c), a rough surface is seen in the sample of test A20. This observation implies that a substantial amount of (large) doloma and periclase grains were dissolved or washed away into the molten slag.

In order to examine the slag infiltration level in MgO-doloma refractory samples, the Al_2O_3 content in the tested refractory finger was measured as a function of the distance from the slag/refractory sample interface by SEM-EDS analyses of the refractory areas with selected scans covering ~ 2000 μm^2 per analysis. The region with an Al_2O_3 content in excess of 1.0 wt pct is considered to be the slag infiltrated refractory part, since the as-delivered refractory contains only ~0.5 wt pct Al_2O_3 (Table II). The measured Al_2O_3 contents in the worn refractory fingers with the distance from the refractory surface are shown in Figure 5. More than

Table III. Chemical Compositions of the Phases in the Magnesia-Doloma Refractory, as Determined by SEM-EDS (Weight Percent)

	Chemical Composition				
Phase	MgO	CaO	Al_2O_3	SiO_2	Fe_2O_3
Periclase	98.3 ± 0.8	1.1 ± 0.3	—	—	0.6 ± 0.5
Lime	3.2 ± 0.8	96.8 ± 0.8	—	—	—
$3CaO{\cdot}SiO_2$	4.5 ± 1.4	64.7 ± 0.9	0.1 ± 0.1	30.6 ± 0.5	—

Table IV. Chemical Compositions of the Slags before and after Refractory Finger Corrosion Tests, as Determined by EPMA-WDS (Weight Percent)

	Chemical Composition						
Test Number	CaO	SiO_2	MgO	Al_2O_3	ΔCaO*	ΔMgO*	C/S**
A05							
Before	51.2 ± 0.3	38.9 ± 0.2	4.1 ± 0.0	5.4 ± 0.1	1.0	0.0	1.3
After	52.2 ± 0.2	37.4 ± 0.2	4.1 ± 0.0	5.7 ± 0.0			1.4
A10							
Before	50.2 ± 0.5	35.4 ± 0.2	4.7 ± 0.3	10.1 ± 0.3	1.1	1.4	1.4
After	51.3 ± 0.3	33.8 ± 0.1	6.1 ± 0.1	8.9 ± 0.4			1.5
A20							
Before	43.3 ± 0.2	33.0 ± 0.3	5.2 ± 0.0	19.1 ± 0.1	1.2	3.4	1.3
After	44.5 ± 0.1	30.5 ± 0.3	8.6 ± 0.2	16.9 ± 0.1			1.5

*ΔCaO = CaO $pct_{after\ test}$ − CaO $pct_{before\ test}$; ΔMgO = MgO $pct_{after\ test}$ − MgO $pct_{before\ test}$.
**C/S = CaO/SiO_2 mass ratio.

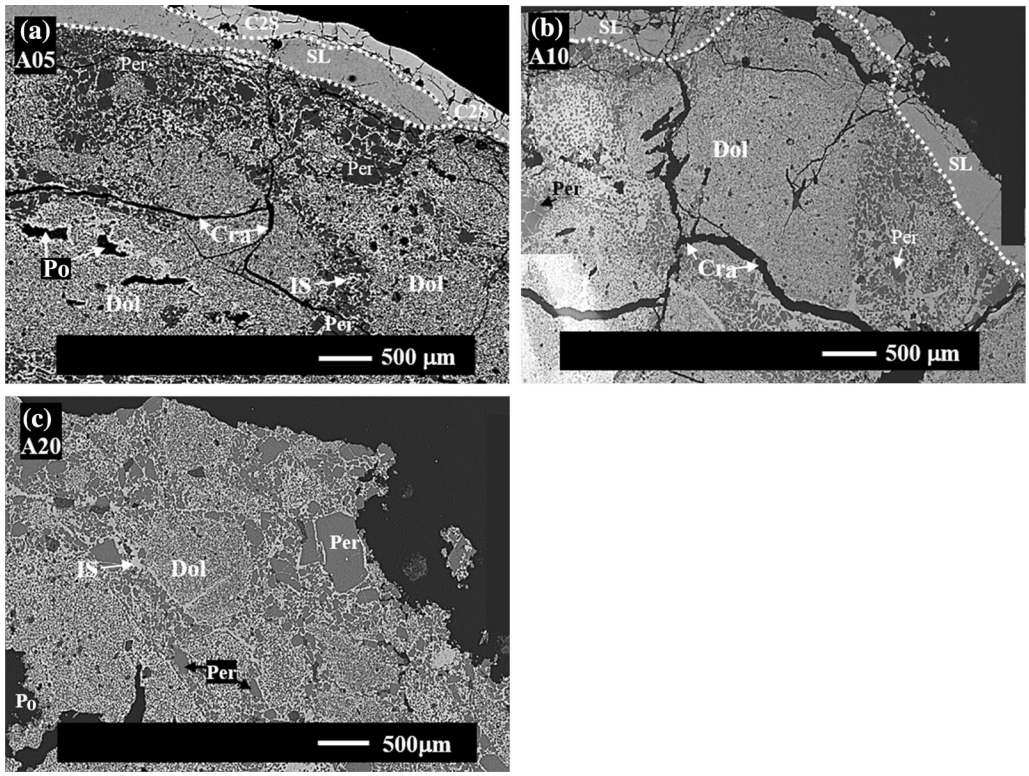

Fig. 4—Overview of the worn refractory samples from the tests with various Al_2O_3 levels: (*a*) 5 wt pct Al_2O_3, (*b*) 10 wt pct Al_2O_3, and (*c*) 20 wt pct Al_2O_3. Dol = doloma grain, Per = periclase (magnesia), IS = infiltrated slag, Po = pore, Cra = crack, SL = slag layer, and C2S = $2CaO{\cdot}SiO_2$. The white dashed line in the images shows the interfaces among the adhered slag layer, the C_2S layer, and the bulk refractory.

Table V. Chemical Composition of the Adhered Slag in Refractory Fingers as Determined by SEM-EDS (Weight Percent)

	Chemical Composition			
Test Number	CaO	SiO_2	Al_2O_3	MgO
A05	49.1	37.5	7.2	6.2
A10	40.8	34.3	12.4	12.5

1.0 wt pct Al_2O_3 was detected at the center position (8 mm) of all three refractory samples. Specifically, the Al_2O_3 contents are located in the range of "1.5 to 2.5 wt pct," "3.0 to 5.5 wt pct," and "5 to 10.0 wt pct" in the refractory samples from tests A05, A10, and A20, respectively. These observations indicate that all refractory fingers were completely infiltrated by CSMA slags in this particular work.

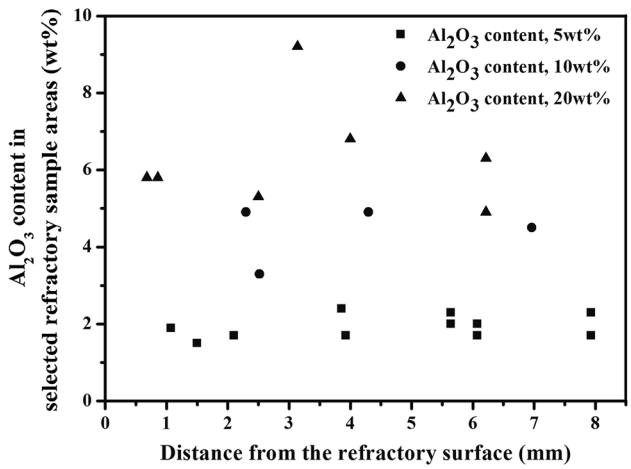

Fig. 5—Measured Al_2O_3 content in worn MgO-doloma fingers as a function of distance from the refractory surface (0 mm), showing the influence of the charged Al_2O_3 content on the slag infiltration.

IV. DISCUSSION

The results showed that the wear of MgO-doloma refractory at the slag/refractory interface is promoted by an increased Al_2O_3 content of the CSMA slags. To understand the influence of the Al_2O_3 level on the CSMA slag/refractory interactions, thermodynamic calculations were performed at 1620 °C. The results are shown in Figure 6. The thermodynamic prediction illustrates that CaO is already saturated in the initial CSMA slags containing 5 and 10 wt pct Al_2O_3 (tests A05 and A10, respectively), leading to the formation of $2CaO{\cdot}SiO_2$ (C_2S) from the slag (Figure 6(a)). The increase of the Al_2O_3 content from 5 to 10 wt pct has an identical C_2S fraction of around 30.0 wt pct

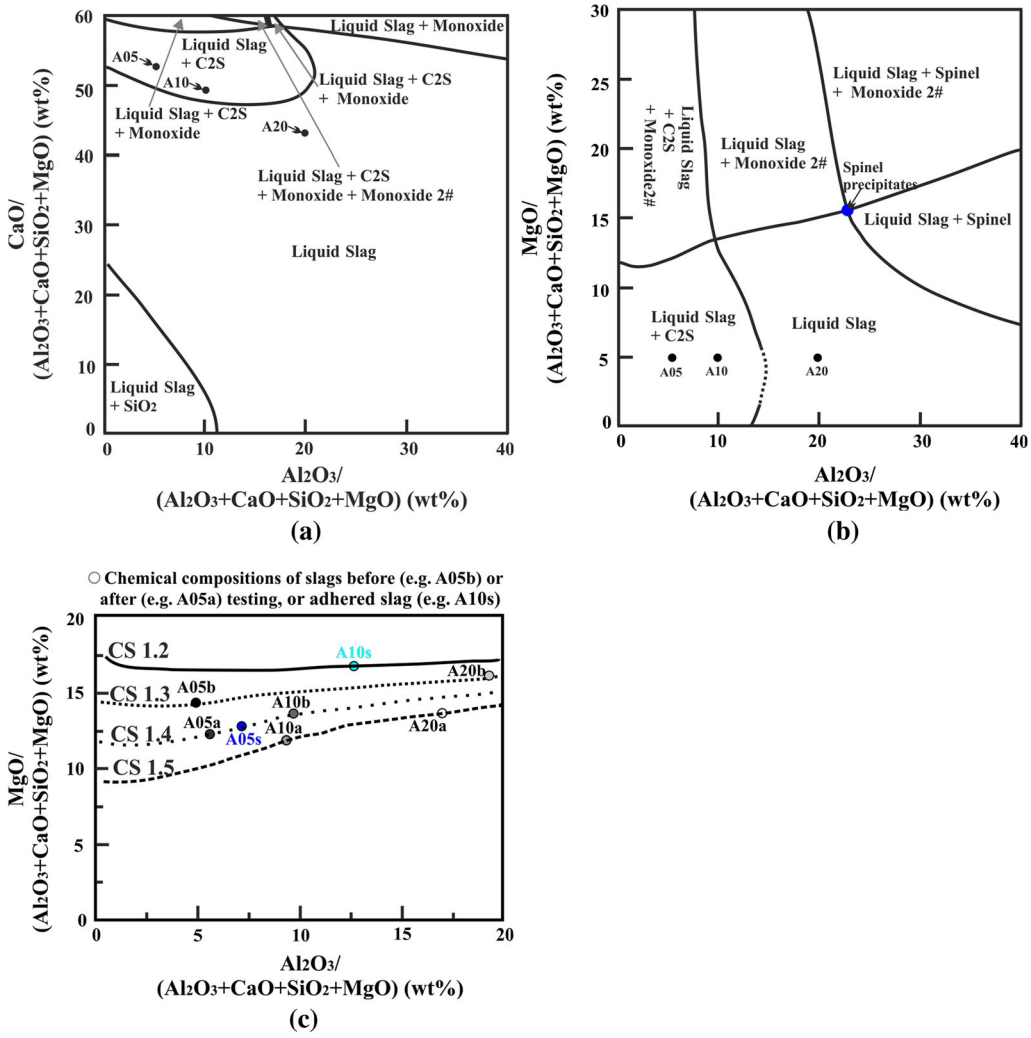

Fig. 6—Phase stability regions at 1620 °C predicted by FactSage, showing the influence of Al_2O_3 on the reaction product formation and the dissolution of (*a*) CaO with a fixed slag MgO content of 5 wt pct, (*b*) MgO with a fixed CaO/SiO_2 mass ratio of 1.4, and (*c*) solubility limits of MgO with varied CaO/SiO_2 mass ratios and Al_2O_3 contents; C2S = $2CaO{\cdot}SiO_2$, Monoxide: CaO-based solid solution, Monoxide 2#: MgO-based solid solution, Spinel = $MgAl_2O_4$ spinel, CS = CaO/SiO_2 mass ratio, and CS 1.2 = CaO/SiO_2 mass ratio of 1.2.

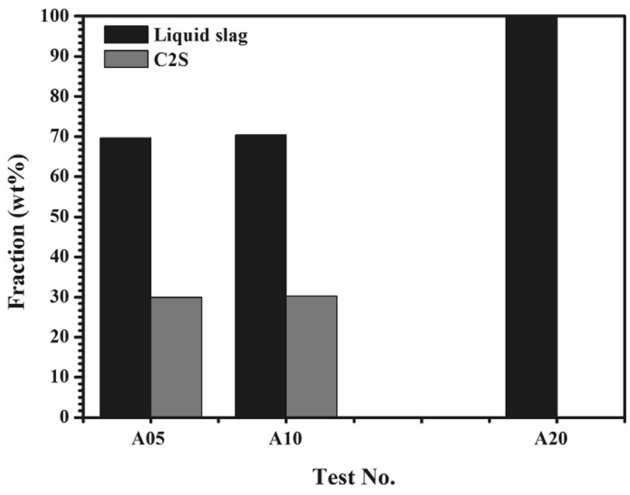

Fig. 7—Phase fraction of the tested slag at 1620 °C predicted by FactSage; C2S = $2CaO{\cdot}SiO_2$.

(Figure 7). As shown in Figure 4, a continuous C_2S layer is observed on the surface of the refractory sample in test A05. The absence of the C_2S layer in test A10 is probably due to the C_2S disintegration during the sampling process. On the other hand, the dissolution of MgO from the refractory continuously occurs in tests A05 and A10 because the adhered slag is not saturated with MgO (Figures 6(b) and (c)). Since a C_2S layer formed between the adhered/frozen slag layer and the bulk slag (Figure 4), the mass transport between the adhered/frozen slag and the bulk slag is physically lowered by the C_2S layer, resulting in increased MgO contents in the frozen slag layers (Table V) and the global slag (Table IV). Additionally, the MgO level in the adhered slag layer increases with increasing the SiO_2 and Al_2O_3 levels due to C_2S formation, since the solubility limit of MgO (MgO saturated) in the adhered CSMA slag having 10 wt pct Al_2O_3 ($MgO_{saturated}$ = 17.0 wt pct ("A10s" in Figure 6(c))) is higher than that containing 5 wt pct

($MgO_{saturated}$ = 12.8 wt pct (“A05s” in Figure 6(c))). Once the Al_2O_3 concentration in the slag is raised to 20 wt pct, the C_2S phase does not form (Figure 4) anymore, due to the high solubility limit of CaO in the slag (60.2 wt pct in Figure 6(a)). Simultaneously, the MgO solubility limit in the bulk CSMA slag further augments to about 15.0 wt pct (Figure 6(b) or “A20b” in Figure 6(c)), resulting in a higher increase of MgO content in the CMSA slag with 20 wt pct (Table IV). As a result, the corrosion mechanism of a slower indirect dissolution changes to a faster direct dissolution of the refractory components, namely, MgO and CaO, at the slag/refractory interface and thus a more severe corrosion rate of the MgO-doloma refractory in test A20 (Figure 4). Because of the increased MgO and CaO content in the slag, the SiO_2 and Al_2O_3 concentrations in the slags are lowered after testing (Table IV). Since the dissolution of refractory components was favored by increasing the Al_2O_3 concentration in CSMA slags (Table IV), the depletion of SiO_2 and Al_2O_3, consequently, was enhanced.

Note in Figure 6(b) that $MgAl_2O_4$ spinel precipitates from CSMA slags with a CaO/SiO_2 ratio of 1.4 when Al_2O_3 and MgO contents are over 22.4 and 15.7 wt pct, respectively. This is consistent with the microstructure observations (Figure 4) that no $MgAl_2O_4$ spinel particles were found in any of the tests.

The increase of the MgO solubility limit in the CSMA slags from 12.0 to 15.7 wt pct by increasing the Al_2O_3 content from 5 to 10 wt pct, consequently, favors the MgO dissolution from the MgO-doloma refractory into the slag, thereby leading to a higher MgO content in the slags containing more Al_2O_3 (Table IV) and an increased overall wear rate of MgO-doloma refractories (Figure 3).

V. CONCLUSIONS

In order to investigate the influence of the Al_2O_3 content in CaF_2-free stainless steel refining slags (CSMA) on the corrosion behavior of magnesia-doloma refractories, static refractory finger corrosion tests were performed under a reducing atmosphere at 1620 °C. Magnesia-doloma refractory finger samples were brought in contact with the CSMA slags with a CaO/SiO_2 ratio of 1.4 and various Al_2O_3 contents, ranging from 5 wt pct to 10 to 20 wt pct. Based on the macroscopic and microstructural observations, the following conclusions can be drawn.

1. The wear of the magnesia-doloma refractories in the CSMA slags with 5 and 10 wt pct Al_2O_3 is predominantly caused by the MgO dissolution into the slags. The increased MgO solubility by enhanced Al_2O_3 concentrations in the CSMA slag is the thermodynamic driving force leading to the accelerated refractory degradation.
2. More serious refractory degradation is observed by increasing the Al_2O_3 content in the CSMA slag to 20 wt pct. This is because the $2CaO{\cdot}SiO_2$ formation at the slag/refractory interface is suppressed, thereby changing the dissolution of CaO and MgO from an indirect method to a direct way, favoring the MgO and CaO dissolution. In addition, both the MgO and CaO solubility limits in the slag are higher compared to the slags with lower Al_2O_3 content.

ACKNOWLEDGMENTS

The authors are grateful for the financial support from Posco and the discussion with Professor J.H. Park, University of Ulsan.

REFERENCES

1. W.E. Lee and S. Zhang: *Int. Mater. Rev.*, 1999, vol. 44, pp. 77–104.
2. A. Buhr: *CN-Refract.*, 1999, vol. 6, pp. 19–30.
3. Z. Wei: *Naihuo Cailiao/Refractor.*, 2002, vol. 36, pp. 224–25 and 28.
4. E.B. Pretorius and R.C. Nunnington: *Ironmak. Steelmak.*, 2002, vol. 29, pp. 133–39.
5. X. Le Coq, B. Dupré, C. Gleitzer, R. Adam, S. François, and P. Tassot: *Steel Res.*, 1990, vol. 61, pp. 593–97.
6. J.H. Park, M.O. Suk, I. Jung, M. Guo, and B. Blanpain: *Steel Res. Int.*, 2010, vol. 81, pp. 2–10.
7. S. Jansson, V. Brabie, and P. Jo: *Ironmak. Steelmak.*, 2008, vol. 35, pp. 99–107.
8. S. Parada, S. Smets, P.T. Jones, M. Guo, W. Patrick, J. Weytjens, and G. Heylen: *Ironmak. Steelmak.*, 2003, vol. 30, pp. 33–39.
9. R.A. Mattila, J.P. Vatanen, and J.J. Härkki: *Scand. J. Metall.*, 2002, vol. 31, pp. 241–45.
10. L. Chen, A. Malfliet, P.T. Jones, B. Blanpain, and M. Guo: *Ceram. Int.*, 2015, vol. 42, pp. 743–51.
11. Y. Satyoko and W.E. Lee: *Br. Ceram. Trans.*, 1999, vol. 98, pp. 261–65.
12. H. Nakada and K. Nagata: *ISIJ Int.*, 2006, vol. 46, pp. 441–49.
13. M. Guo, P.T. Jones, S. Parada, E. Boydens, J. Van Dyck, B. Blanpain, and P. Wollants: *Ceram. Int.*, 2006, vol. 33, pp. 3831–43.
14. M. Guo, P.T. Jones, S. Parada, E. Boydens, J.V. Dyck, B. Blanpain, and P. Wollants: *J. Eur. Ceram. Soc.*, 2006, vol. 26, pp. 3831–43.
15. L. Chen, S. Li, P.T. Jones, M. Guo, B. Blanpain, and A. Malfliet: *J. Eur. Ceram. Soc.*, 2016, vol. 36, pp. 2119–32.
16. C.W. Bale, E. Bélisle, P. Chartrand, S.A. Decterov, G. Eriksson, A.E. Gheribi, K. Hack, I. Jung, Y. Kang, J. Melançon, A.D. Pelton, S. Petersen, C. Robelin, J. Sangster, P. Spencer, and M. Van Ende: *Calphad*, 2016, vol. 55, pp. 1–19.
17. Verein Deutscher Eisenhüttenleute (VDEh): *Slag Atlas*, Verlag Stahleisen GmbH, Düsseldorf, 1995, pp. 156–61.
18. L. Chen, M. Guo, H. Shi, S. Huang, P.T. Jones, B. Blanpain, and A. Malfliet: *J. Eur. Ceram. Soc.*, 2016, vol. 36, pp. 1821–28.
19. L. Chen, A. Malfliet, J. Vleugels, B. Blanpaina, and M. Guo: *Corros. Sci.*, 2018, vol. 136, pp. 409–17.
20. R.C. Doman, J.B. Barr, R.N. McNally, and A.M. Alper: *J. Am. Ceram. Soc.*, 1963, vol. 46, pp. 313–16.